[Chem. Pharm. Bull. 36(8)2742—2749(1988)]

Effect of the Solubilized State of Tetraphenylporphyrin as a Photosensitizer on the Photooxidation of Methyl Orange in Sodium Dodecyl Sulfate Solution

MASAYUKI NAKAGAKI,[a] KAZUHIRO INOUE,[b] HIROAKI KOMATSU,*,[b] TETSUROU HANDA[b] and KOICHIRO MIYAJIMA[b]

Hoshi University,[a] Ebara, Shinagawa-ku, Tokyo 142, Japan and Faculty of Pharmaceutical Sciences, Kyoto University,[b] Yoshida-shimoadachi-cho, Sakyo-ku, Kyoto 606, Japan

(Received November 9, 1987)

The effect of concentration of sodium dodecyl sulfate (SDS) on the efficiency of photooxidation of methyl orange (MO) sensitized with tetraphenylporphyrin (TPP) in SDS aqueous solution was investigated. Below the critical micelle concentration of SDS–TPP mixed solution (cmc_{mix}), TPP was solubilized as an oligomer complex composed of one or plural TPP molecules and plural SDS ones; only the oligomer complex composed of one TPP molecule and plural SDS ones (TPPm–SDSs complex) among the oligomer complexes contributed to the efficient photooxidation of MO. Above the cmc_{mix}, however, the reaction efficiency decreased with increase in the SDS concentration. Above the cmc_{mix}, all the TPP molecules were not always solubilized without aggregating among themselves in the micellar phase and some of the TPP molecules were solubilized as TPPm–SDSs complexes in the aqueous phase. With increase in the SDS concentration, the TPPm–SDSs complexes were absorbed into the micelle and TPP monomer was increased in the micellar phase, where TPP had a lower reaction efficiency than TPP solubilized as a TPPm–SDSs complex due to the less polar environment in the micellar phase. Thus, above the cmc_{mix}, the diminution of the reaction efficiency with increasing SDS concentration could be ascribed to the decrease in the amount of TPP monomer solubilized as a TPPm–SDSs complex.

Keywords——singlet oxygen; tetraphenylporphyrin; methyl orange; sodium dodecyl sulfate; photooxidation; micellar solution; micellar environment

Photooxidations employing porphyrin derivatives as photosensitizers have been utilized in the photochemotherapy of various tumors.[1] In our previous studies, photooxidation of methyl orange (MO) sensitized with tetraphenylporphyrin (TPP) in a variety of surfactant micelles was carried out as a model of biological systems, and the effects of the microenvironment around the sensitizer on the photooxidation were investigated.[2] It was found that the photooxidation of MO is mediated by the potent oxidizing agent, singlet oxygen.[2b] In one study,[2d] it was noted that the reaction efficiency below the critical micelle concentration (cmc) of sodium dodecyl sulfate (SDS) was higher than that above the cmc. However, examination of the reaction efficiency in the regions of high SDS concentration was not undertaken. In the present experiments, we investigated the photooxidation of MO over a wide concentration region including a high SDS concentration, and the relation between the dissolved states of the TPP molecules and their reaction efficiencies was evaluated on the basis of spectrophotometric determination of the TPP monomer concentrations.

Experimental

Materials——The anionic surfactant, SDS, was obtained from Nakarai Chemical Co., Ltd. The surfactant was washed with ether and recrystallized twice from hot ethanol. The surface tension *vs.* concentration curve for the

aqueous SDS solution yielded no minimum around the cmc. Meso-α,β,γ,δ-tetraphenylporphyrin (TPP) was purchased from Dojindo Laboratories. The purity of the TPP was monitored by thin layer chromatography on Silica gel 70 with *n*-hexane–acetone (1 : 1, v/v) as the eluting solvent. A single spot was obtained. MO was obtained from Wako Pure Chemical Industries Ltd. Tris(hydroxymethyl)aminomethane (Tris) of analytical grade was used as received. Water was doubly distilled from a quartz still.

Measurements——The sample solution was prepared by the following procedures. Aliquots of stock solutions of TPP in acetone and of SDS in water were mixed. The solvent of the mixed solution was evaporated off at 40 °C and the residue was dissolved in 1 mM Tris–HCl buffer (pH 7.3) solution containing 2.1 μM MO.

Irradiation was carried out under a Kondo-Sylvania 1 kW tungsten–halogen lamp. A Toshiba KL-42 interference filter (transmittance characteristics: $\lambda_{max}=417.5$ nm, half wavelength = 18.0 nm) was used to obtain monochromatic light. The sample solution contained in a quartz cell was kept at 25 °C by circulation of thermostated water, and it was stirred well with a magnetic stirrer during the irradiation.

The absorption spectra were measured with a Shimadzu UV-265FW spectrophotometer. The fluorescence intensities of TPP excited at 417 nm were monitored at 653 nm using a Jasco FP-550 spectrofluorometer at 25 °C.

Full details of the sample preparation and measurements have been given elsewhere.[2d]

Analysis

Calculation of the Amounts of Photons Absorbed by TPP Monomer in Unit Time *Q*——In our previous studies, based on the assumption that the Q value is proportional to the fluorescence intensity of TPP (F), the photooxidation efficiencies of MO were discussed exclusively by using the F value. Above 1 μM TPP, however, the linear relationship between Q and F no longer holds good due to interior shielding effects. In the present study, the Q value was calculated differently.

The Q value may be represented as follows[3]:

$$Q=\int_0^L I_0 A_{TPP} 10^{-A_T x} dx$$

$$=\frac{I_0 A_{TPP}}{\ln 10 A_T}(1-10^{-LA_T}) \quad (1)$$

where $A_T=A_{TPP}+A_{MO}$ and I_0 is the intensity of light incident upon the reaction cell, L the light-path length of the cell, A_{TPP} the total absorbance at the absorption maximum (at 417 nm) of TPP, and A_{MO} the absorbance of MO at 417 nm. When the SDS concentration was sufficiently high to solubilize all the TPP as monomers without aggregating in the micellar phase, the absorption spectra of TPP had a sharp absorption maximum at 417 nm, as shown in Fig. 1a. However, when the SDS concentration was not so high, the absorbance of TPP at 417 nm was small and the absorption band became broad, as shown in Fig. 1b. This broadening was clearly visible on the difference spectrum between Fig. 1a and b, as shown in Fig. 1c. The appearance of such a broad band indicated the formation of TPP aggregates, *i.e.*, dimer, trimer, *etc.*, in the SDS aqueous solution. The photons absorbed by these TPP aggregates were

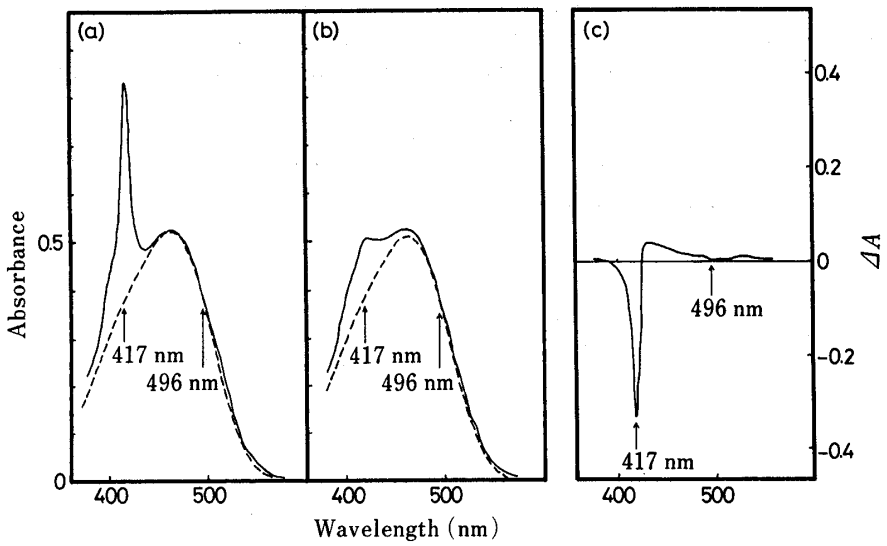

Fig. 1. Absorption Spectra (a and b) and Difference Absorption Spectrum (c) of 21 μM MO in SDS Solutions with 1.0 μM TPP (——) and without TPP (----)
(a) [SDS] = 20 mM; (b) [SDS] = 8 mM.

unavailable for the reaction.

It is necessary for accurate calculation of the Q value and of the absorbance of TPP monomer at 417 nm (A_{TPPm}) to subtract the absorbance of the TPP aggregates (A_{TPPa}) from A_{TPP}: $A_{TPPm}=A_{TPP}-A_{TPPa}$. Since the TPP aggregates do not fluoresce, the A_{TPPm} values were estimated by using the F values. Plots of A_{TPP} against the total TPP concentration ($[TPP]_T$) in 20 mM SDS solution showed a linear relationship at $[TPP]_T \leqq 3\,\mu M$, indicating that all the TPP is solubilized without aggregating. From the slope of this line, the molar extinction coefficient of TPP monomer in the micellar phase was determined as $\varepsilon_{417\,nm}=4.7\times10^5\,M^{-1}\cdot cm^{-1}$.

It was found that the F value was not proportional to A_{TPP} at $[TPP]_T \leqq 3\,\mu M$ in 20 mM SDS solution from plots of A_{TPP} against F. When the emission arising from the central part of the exciting region located between $L/2-d$ and $L/2+d$ cm in the sample cell is detected in a direction perpendicular to the exciting beam, the correlation between F and A_{TPP} can be expressed as follows[3]:

$$F=\frac{I_0\alpha\beta}{\ln 10}10^{-(1/2)A_{TPP}}(10^{dA_{TPP}}-10^{-dA_{TPP}}) \tag{2}$$

where $L=1$ cm in this study. Here, α is the fluorescence yield of TPP and β a characteristic parameter of our fluorometer. Since the d value is very small, Eq. 2 can be rewritten approximately as follows:

$$F=2I_0\alpha\beta dA_{TPP}10^{-(1/2)A_{TPP}} \tag{3}$$

and

$$\ln F=\ln(2I_0\alpha\beta d)+\ln A_{TPP}-\frac{1}{2}(\ln 10)A_{TPP} \tag{4}$$

Figure 2 shows plots of $\ln F$ against $\ln A_{TPP}-(1/2)(\ln 10)A_{TPP}$ according to Eq. 4. By extrapolating the linear $\ln F$ *vs.* $\ln A_{TPP}-(1/2)(\ln 10)A_{TPP}$ plots to $\ln A_{TPP}-(1/2)(\ln 10)A_{TPP}=0$, the $\alpha\beta d$ value was estimated to be 3.93 by using $I_0=3.21\times10^{15}$ quanta$\cdot s^{-1}$ as determined by ferrioxalate chemical dosimetry.[2d] The best fit between Eq. 2 and the observed data, which represent the relation between F and A_{TPP}, was obtained at $d=0.3$ cm. By substituting the values of $\alpha\beta$ and d into Eq. 2, we have

$$F=0.569\times10^{-(1/2)A_{TPP}}(10^{0.3A_{TPP}}-10^{-0.3A_{TPP}}) \tag{5}$$

A_{TPP} values were obtained from the F values by using Eq. 5, and the Q values were then estimated from the resultant A_{TPP} values by using Eq. 1.

Determination of the Apparent Rate Constant k——A mechanism for the photooxidation was proposed in our previous paper: it was found that MO is oxidized by singlet oxygen, which is produced by the reaction of oxygen with TPP in the triplet excited state.[2b] The absorption spectra of TPP and MO overlap with each other in the region from 360 to 500 nm, as shown in Fig. 1. The decomposition of MO was monitored from the decrease in absorbance at 496 nm, where the absorbance of TPP is trivial. Since the ratio of the absorbance of MO at 417 nm to that at 496 nm is constant, the time course of the absorbance of MO at 417 nm was obtained from that of MO at 495 nm. The time course of the absorbance of TPP was evaluated by subtracting the absorbance of MO at 417 nm from the total absorbance of the sample solution at 417 nm. This absorbance occasionally contains the absorbance of TPP aggregates. In such a case, the initial value of A_{TPPm} ($A_{TPPm(0)}$) is calculated from the initial F value by using Eq. 5 and the A_{TPPm} after t s' irradiation ($A_{TPPm(t)}$) can be calculated according to the following equation.

$$A_{TPPm(t)}=A_{TPP(t)}-(A_{TPP(0)}-A_{TPPm(0)}) \tag{6}$$

where $A_{TPP(0)}$ is the initial A_{TPP}, and $A_{TPP(t)}$ is the A_{TPP} after t s' irradiation based on the assumption that the

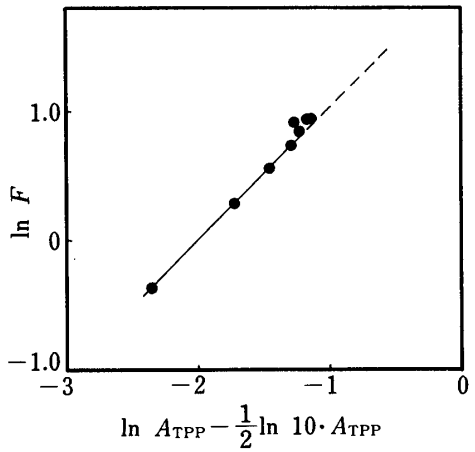

Fig. 2. Plots of $\ln F$ against $\{\ln A_{TPP}-(1/2)(\ln 10)\times A_{TPP}\}$

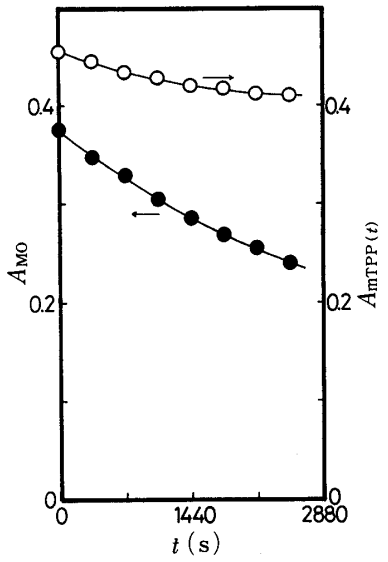

Fig. 3. Time Courses of the Absorbance of MO at 417 nm (A_{MO}) and Absorbance of TPP Monomer after ts' Irradiation ($A_{mTPP(t)}$)
●, A_{MO}; ○, $A_{mTPP(t)}$.

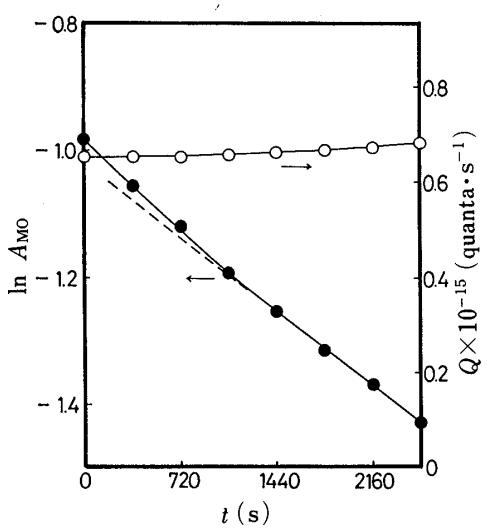

Fig. 4. Time Course of ln A_{MO} (●) and Q (○)

absorbance of TPP aggregates remains almost constant during the irradiation. Figure 3 shows the time courses of A_{MO} and $A_{TPPm(t)}$. Not only MO but also TPP monomer underwent decomposition.

As can be seen from Eq. 1, the quantity Q is a function of both A_{MO} and $A_{TPPm(t)}$, and Q changes with the irradiation time. As shown in Fig. 4, however, the Q value fortunately barely changed during the irradiation, because the decrease in $A_{TPPm(t)}$ causes a decrease in Q but the decrease in A_{MO} results in an increase in Q. The change in Q value amounted to less than 5% of the initial value. There was a linear relationship between ln A_{MO} and the irradiation time t except during the initial period of the irradiation time. The slope of the straight line was employed as the apparent rate constant k. The degradation of MO is given by[2d]

$$-\frac{d[MO]}{dt}=k[MO] \tag{7}$$

and

$$\ln[MO]=\ln[MO]_0-kt \tag{8}$$

where $[MO]_0$ is the initial concentration of MO. Since the production processes of singlet oxygen are much faster than the oxidation process of MO with singlet oxygen. $[^1O_2]$ is proportional to the concentration of TPP in the singlet excited state and also to Q.[2] The rate constant k is

$$k=k'[^1O_2]=k'\gamma[TPPm^*]=k'\delta Q \tag{9}$$

where k' is the second-order rate constant, [TPPm*] the concentration of TPP monomer in the excited state, and the quantities γ and δ are constants.

The average value of Q ($\bar{Q}$) was calculated in the time region where ln A_{MO} varied linearly with the irradiation time t.

Results

Figure 5 shows [TPPm] in the micellar phase as a function of the SDS concentration at various TPP concentrations. The cmc values of the SDS–TPP mixed solution (cmc_{mix}), shown by the arrows in Fig. 5, were determined as 7 mM based on measurements of the surface tension of the mixed solutions.[2d] These plots indicate that below the cmc_{mix}, some of the TPP molecules are solubilized without aggregating among themselves in the aqueous phase. It has been suggested by many workers that below the cmc of SDS, water-insoluble dye molecules are solubilized by forming complexes with some SDS molecules, that is, by forming pre-

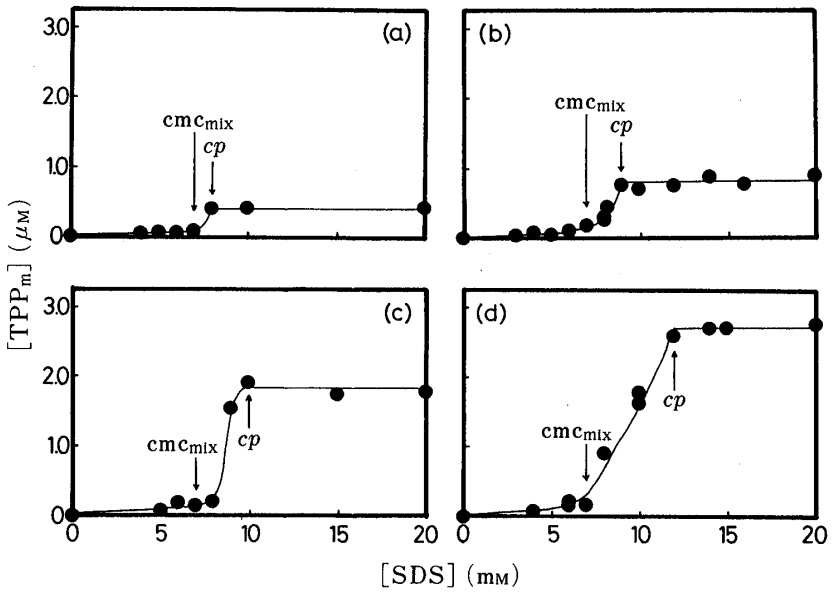

Fig. 5. Concentration of TPP Monomer ([TPPm]) as a Function of SDS Concentration at TPP Concentrations ($[TPP]_T$) of 0.5 μM (a), 1.0 μM (b), 2.0 μM (c) and 3.0 μM (d)

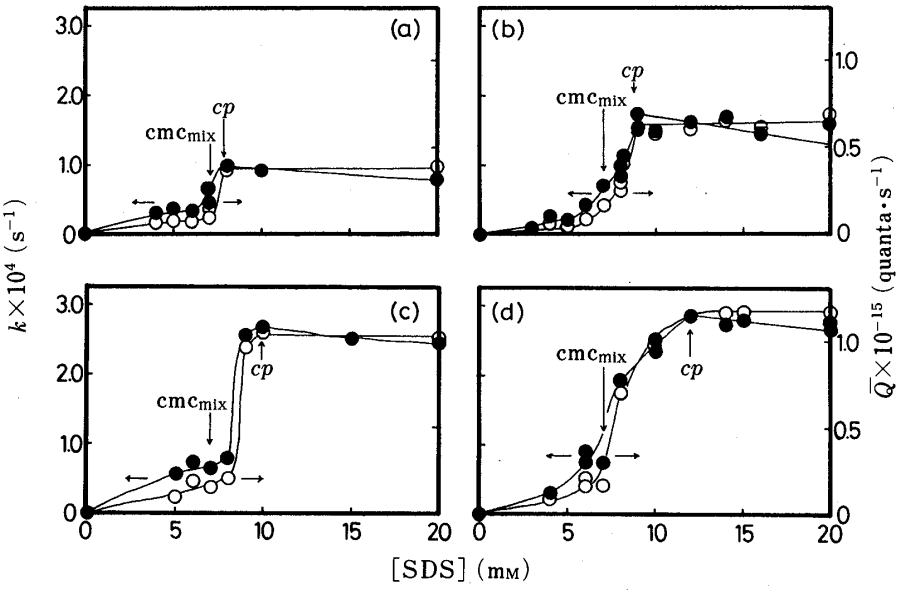

Fig. 6. Values of k (●) and $\bar{Q}$ (○) as a Function of SDS Concentration at Total TPP Concentrations ($[TPP]_T$) of 0.5 μM (a), 1.0 μM (b), 2.0 μM (c) and 3.0 μM (d)

micelles.[4-7] With further increase in the SDS concentration, the [TPPm] value increased and reached a maximum at a specific SDS concentration (*cp*). The [TPPm] became constant above this *cp*. Since the *cp* value increased with $[TPP]_T$, as shown in Fig. 5, the *cp* value represents the minimum SDS concentration at which all the TPP molecules are solubilized without aggregating among themselves in the micellar solution. The increase in [TPPm] at $cmc_{mix} < [SDS] < cp$ indicates that there is a dissociation process of TPP aggregates into monomer.

The values of k and $\bar{Q}$ as a function of the SDS concentration at various TPP concentrations are shown in Fig. 6. The change in $\bar{Q}$ value corresponds to that in the [TPPm] value, but above the *cp* the k value gradually decreased with increase in the SDS

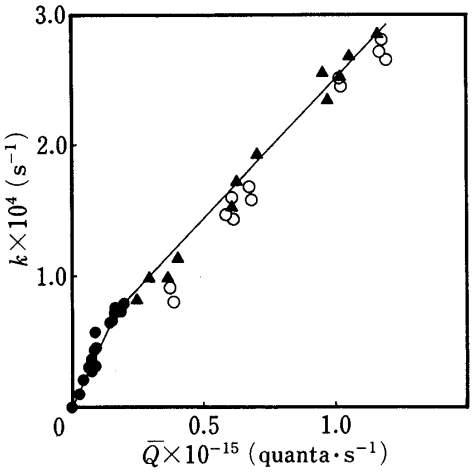

Fig. 7. Plots of k Value against the Average of $Q(\bar{Q})$

●, [SDS]≦cmc_{mix}; ▲, cmc_{mix}<[SDS]<cp; ○, cp≦[SDS]≦20 mM.

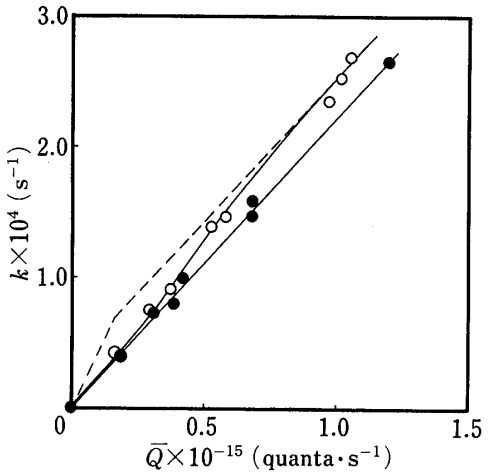

Fig. 8. Plots of k Value against $\bar{Q}$ at 10 mM (○) and 20 mM SDS (●)

The dashed lines are the same as the lines depicted in Fig. 7.

concentration. Figure 7 gives the plots of the k value as a function of the $\bar{Q}$ value at various $[TPP]_T$. The plots below the cp (represented by closed circles and triangles) yielded two straight lines having an intersection at the cmc_{mix} and the slope was larger at [SDS]≦cmc_{mix} than at cmc_{mix}<[SDS]<cp. Since TPP monomer is not solubilized in the micellar phase below the cmc_{mix}, the slope in this region of SDS concentration corresponds to the reaction efficiency ($k'\delta$ in Eq. 9) of TPP monomer solubilized by forming an oligomer complex composed of one TPP molecule and plural SDS ones (TPPm–SDSs complex) in the aqueous phase. At cmc_{mix}<[SDS]<cp, a linear relation exists between the k and $\bar{Q}$ values and the slope is different from the slope below the cmc_{mix}, indicating that in this region of SDS concentration the TPPm–SDSs complex concentration does not change and the TPP monomer in the micellar phase increases, that is, aggregates of TPP molecules dissociate into monomer in the micellar phase with increasing SDS concentration. Thus, the slope at cmc_{mix}<[SDS]<cp corresponds to the reaction efficiency ($k'\delta$ in Eq. 9) of TPP monomer in the micellar phase.

Above the cp, the plots (represented by open circles in Fig. 7) became deviated downwards from the straight line at cmc_{mix}<[SDS]<cp (shown as closed triangles). Such deviation indicates a change in the dissolved states of TPP monomer above the cp, since [TPPm] does not decrease and is constant, as shown in Fig. 5. To confirm the change in the dissolved states of TPP monomer, we assumed that at cmc_{mix}<[SDS]<cp the TPPm–SDSs complexes remained in the aqueous phase and the TPPm–SDSs complex concentration was constant, and that above the cp the TPPm–SDSs complexes were absorbed into the micelle, while the TPP monomers in the micelle alone existed in the micellar solution at a sufficiently high SDS concentration relative to the TPP concentration. In order to verify these assumptions, the relations between k and $\bar{Q}$ were studied at a sufficiently high SDS concentration (at 20 mM SDS) relative to the cp and in the region of TPP concentration from 0 to 3.0 μM. As shown in Fig. 8, the plots (represented by closed circles) of k against $\bar{Q}$ at 20 mM SDS fell on a straight line through the origin, the slope of which was comparable with that of the line (upper part of the dashed line in Fig. 8) at cmc_{mix}<[SDS]<cp in Fig. 7. On the other hand, the plots (represented by open circles) at 10 mM SDS formed a curved line: they tended to approach the solid line in the region of low TPP concentration and the dashed line at a high TPP concentration. This suggests the validity of the above assumptions.

From the above results, the reaction efficiencies were evaluated by dividing the SDS concentration into four regions: [SDS]≦cmc_{mix}, cmc_{mix}<[SDS]<cp, cp≦[SDS] (<20 mM)

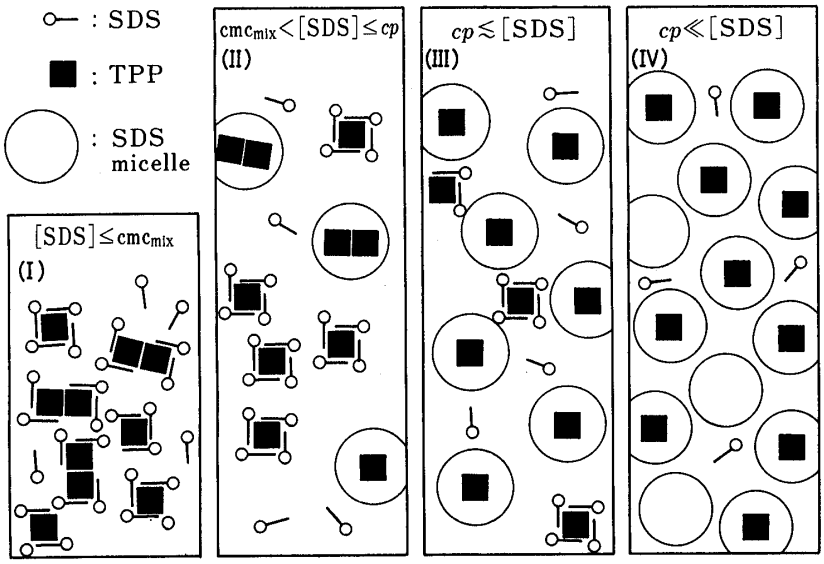

Fig. 9. Dissolved States of TPP Molecules in SDS Aqueous Solution

and $cp \ll$ [SDS] (20 mM $\leqq$ [SDS] in our studies), as illustrated in Fig. 9.

Discussion

Below the cmc_{mix}, TPP molecules are solubilized as complexes composed of one or plural TPP molecules and plural SDS ones and the TPPm–SDSs complex concentration increases with SDS concentration (Fig. 9(I)). At $cmc_{mix} < [SDS] < cp$, with increase in the SDS concentration the TPP aggregates in the micellar phase (*e.g.* dimer TPP in Fig. 9) dissociate into monomer and the TPP monomer concentration in the micellar phase increases but the TPPm–SDSs complex concentration in the aqueous phase remains constant (Fig. 9(II)). The total amount of light absorbed by all the TPP monomer per unit time ($\bar{Q}$) can be expressed as follows:

$$\bar{Q} = \bar{Q}_b + \bar{Q}_m \tag{10}$$

where $\bar{Q}_b$ and $\bar{Q}_m$ are the amounts of light per unit time absorbed by TPP solubilized as a TPPm–SDSs complex in the aqueous phase and by TPP monomer in the micellar phase, respectively. The apparent rate constant k is given by

$$k = k_b \bar{Q}_b + k_m \bar{Q}_m \tag{11}$$

where k_b and k_m are parameters ($k'\delta$ in Eq. 9) corresponding to the reaction efficiency of TPP monomer per single photon. These quantities are associated with TPP solubilized as a TPPm–SDSs complex in the aqueous phase and with TPP monomer in the micellar phase, respectively. Below the cmc_{mix}, k is proportional to $\bar{Q}$, as follows:

$$k = k_b \bar{Q}_b = k_b \bar{Q} \tag{12}$$

because $\bar{Q}_m = 0$. At $cmc_{mix} < [SDS] < cp$, the $\bar{Q}_b$ value is constant at $\bar{Q}_{b\,max}$, which is comparable to the $\bar{Q}_b$ value at the cmc_{mix} or cp. $\bar{Q}$ and k can be expressed as follows:

$$\bar{Q} = \bar{Q}_{b\,max} + \bar{Q}_m \tag{13}$$

and

$$\begin{aligned} k &= k_b \bar{Q}_{b\,max} + k_m \bar{Q}_m \\ &= (k_b - k_m)\bar{Q}_{b\,max} + k_m \bar{Q} \end{aligned} \tag{14}$$

Equation 14 describes the relation between $\bar{Q}$ and k in Fig. 7 (the plots represented by closed circles and triangles), and the values of k_b and k_m were determined as $k_b = 4.29 \times 10^{15}$ quanta^{-1} and $k_m = 2.17 \times 10^{15}$ quanta^{-1} from the slopes.

The value of k_b was thus about twice as large as that of k_m. The difference between their values has been discussed in our previous paper[2d]; all singlet oxygen produced by the TPPm–SDSs complex interacts with MO in the aqueous phase. Some of the singlet oxygen produced by the TPP monomer in the micellar phase interacts with MO adsorbed on the micellar surface. However, it has been found that the activity of the singlet oxygen is decreased in a less polar environment such a micellar phase.[2a,b] The singlet oxygen produced in the micellar phase can therefore hardly oxidize MO in the less polar environment on the micellar surface and is rather inactivated by MO adsorbed on the micellar surface.[2a,b,d]

In our previous paper,[2d] it was assumed that the concentration of TPPm–SDSs complex was constant above the *cp*. In the present study, however, it was found that the concentration of TPPm–SDSs complex gradually decreased with increase in the SDS concentration and all the TPP was solubilized as monomer in the micellar phase at 20 mM SDS (Fig. 9(IV)). Since TPP solubilized as TPPm–SDSs complex is absorbed into the micelle with increasing SDS concentration, the $\bar{Q}$ value is constant at $\bar{Q}_{max}$ above the *cp* and the k value decreases from $(k_b - k_m)\bar{Q}_{b\,max} + k_m\bar{Q}_{max}$ to $k_m\bar{Q}_{max}$. The data at 10 mM SDS in Fig. 8 also support the validity of the above analysis.

When the TPP concentration is very small relative to the SDS concentration, all TPP molecules are solubilized as the monomer without aggregating among themselves in the micellar phase, as illustrated in Fig. 9(IV), and the relationship between k and $\bar{Q}$ becomes:

$$k = k_m\bar{Q} \tag{15}$$

On the other hand, when the TPP concentration is not so small compared to the SDS concentration, some of the TPP molecules cannot be solubilized in the micellar phase and they are solubilized as TPPm–SDSs complexes in the aqueous phase. The relationship between k and $\bar{Q}$ then becomes:

$$k = (k_b - k_m)\bar{Q}_{b\,max} + k_m\bar{Q} \tag{16}$$

In conclusion, even above the cmc_{mix}, all the TPP molecules are not always solubilized as the monomer without aggregating among themselves in the micellar phase. When the SDS concentration is not sufficiently higher than the TPP concentration, TPP is solubilized as a TPPm–SDSs complex in the aqueous phase. The TPP forming the TPPm–SDSs complexes contributes to the high efficiency of the MO photooxidation not only below but also above the cmc_{mix}.

References

1) D. Kessel and T. J. Dougherty (eds.), "Porphyrin Photosensitization," Vol. 160, Adv. Exper. Med. Biol., Plenum Press, New York and London, 1981, p. 1; D. R. Doiron and C. J. Gomer (eds.), "Porphyrin Localization and Treatment of Tumors," Alan R. Liss, Inc., New York, 1984, p. 41; D. Kessel (ed.), "Methods in Porphyrin Photosensitization," Vol. 193, Adv. Exper. Med. Biol., Plenum Press, New York and London, 1985, p. 3.
2) *a*) M. Nakagaki, M. Sakai and T. Handa, *Chem. Pharm. Bull.*, **32**, 4241 (1984); *b*) T. Handa, M. Sakai and M. Nakagaki, *ibid.*, **33**, 2618 (1985); *c*) T. Handa, H. Takeuchi, H. Takagi, Y. Kawashima, H. Komatsu and M. Nakagaki, *J. Pharmacobio-Dyn.*, **10**, s-125 (1987); *d*) M. Nakagaki, K. Inoue, H. Komatsu, T. Handa and K. Miyajima, *Chem. Pharm. Bull.*, **36**, 1 (1988).
3) Th. Förster, "Fluoreszenze Organischer Verbindungen," Vandenhoeck & Ruprecht, Gottingen, 1951, p. 1.
4) P. Hambright, "Porphyrins and Metalloporphyrins," ed. by K. M. Smith, Elsevier Scientific Publishing Company, Amsterdam, 1975, p. 265.
5) E. Lohoczki and J. Hevesi, *Dokl. Akad. Nauk SSSR*, **206**, 1158 (1972).
6) P. Mukerjee and K. J. Mysels, *J. Am. Chem. Soc.*, **77**, 2937 (1955).
7) H. Sato, M. Kawasaki, K. Kasatani, N. Nakashima and K. Yoshihara, *Bull. Chem. Soc. Jpn.*, **56**, 3588 (1983).